A00-39948

AIAA-2000-4341

G-Force: The Design Of An Unlimited Class Reno Racer

E. Ahlstrom, R. Gregg,
J. Vassberg & A. Jameson

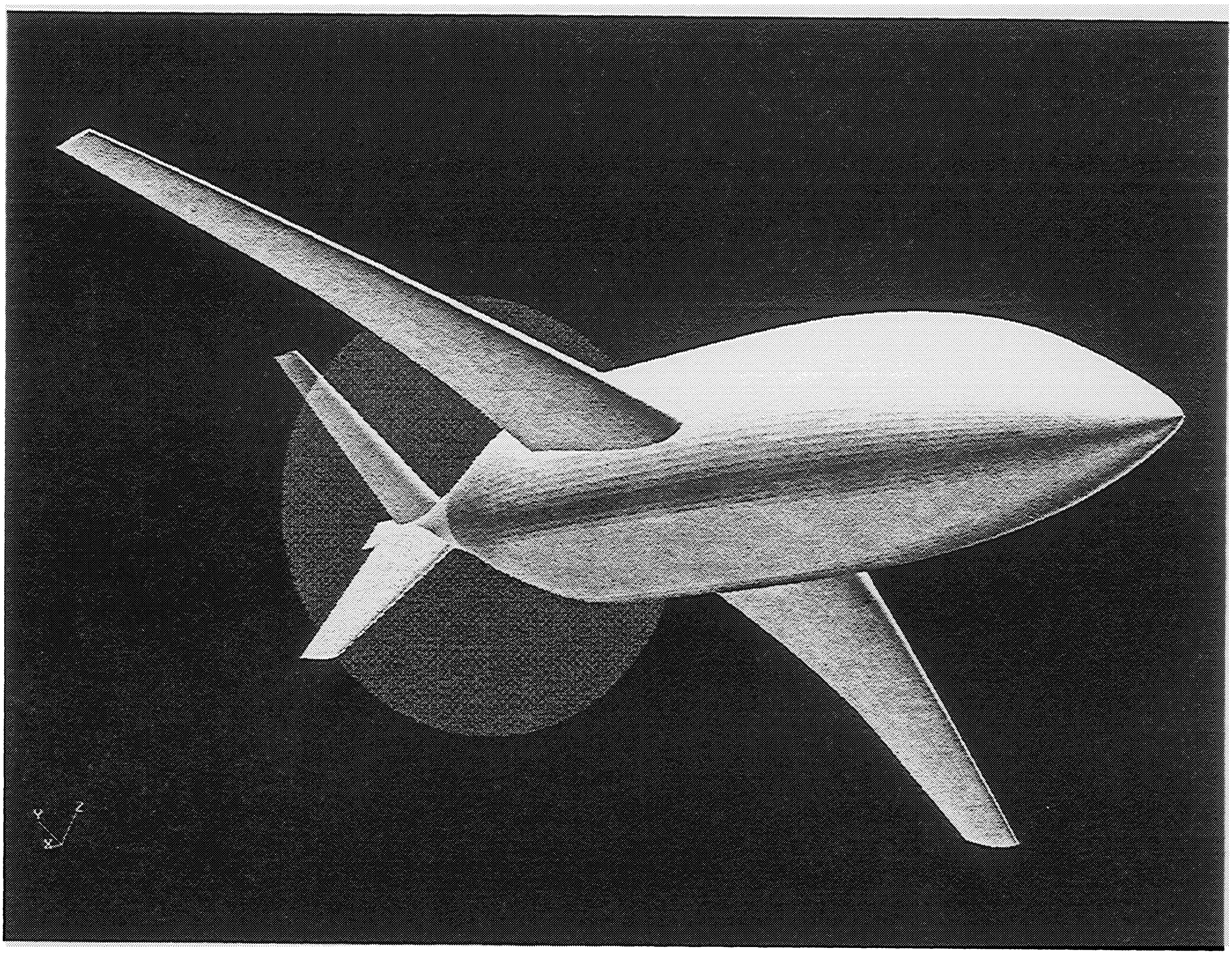

18th AIAA Applied Aerodynamics Conference
14-17 August 2000 / Denver, CO

G-Force: The Design Of An Unlimited Class Reno Racer

E. Ahlstrom* (Star Aerospace LLC), R.D. Gregg† (Independent Consultant), J.C. Vassberg‡ (Independent Consultant), & A. Jameson§ (Stanford University)

Introduction

In May 1999, Renaissance Research contracted Star Aerospace LLC to design an Unlimited Class racing aircraft. At present, modified piston-prop fighters designed before and during WWII dominate this form of racing. These aircraft are now over 50 years old and have very little service life left. Engine reliability is so poor that a winning Unlimited aircraft will spend less than one hour at full throttle between engine rebuilds. Overhaul costs range from $150,000 to $250,000 for the 1940's technology engines due to the disappearing parts supply. Finally, the historic value of flyable WWII fighters has increased to over $1,000,000, well beyond the level affordable for racing use. Replicas of existing designs face the same engine limitations as their predecessors. If Unlimited racing is to continue through the next decade, new Unlimited race plane designs are required.

Previous attempts in the last twenty years at fielding a dedicated Unlimited racer have been limited to two conventional designs (one single-engine and one twin), and one warbird derivative. The single engine aircraft, Tsunami, was basically a downsized version of the P-51. Freed of the military requirements of armament and long range, Tsunami was the first Unlimited to unofficially post a 500 mph lap at the Reno air races. This design did not make use of advances in aerodynamic methods or concepts. Furthermore, it used a Merlin engine with the same dwindling, expensive parts supply as the modified Mustang racers. Unfortunately, Tsunami and pilot were lost in a landing accident in 1991 due to a flap failure, limiting the influence of this design on Unlimited racing.

The twin-engine aircraft, Burt Rutan's Pond Racer, was similar in configuration to the P-38 with twin-engine booms and a center pod cockpit. The small auto racing engines used had never seen continuous duty at over 500 HP and quickly overheated under race conditions where 1000 HP was needed just to be competitive. Engine reliability of this aircraft at Reno continued to be an issue. In three years, this aircraft only finished one low speed Bronze category race coming in second to a stock P-51. The aircraft and the pilot were lost in 1993 after an engine failure.

Last, Miss Ashley II consisted of a replica P-51 fuselage mated to a Lear 23 wing and tail along with a Griffon engine-powering counter rotating propellers. While fast, it suffered a control failure in 1999; the aircraft was destroyed and the pilot lost.

The record of built-for-purpose Unlimited racers is even worse than the aircraft they were supposed to replace. Any new design must address the issues of these failures and prove itself reliable and safe enough to take the place of the tried and true warbirds.

This paper discusses the design work completed for a new Unlimited Class Race Aircraft named the G-Force Racer.

---

* President, Star Aerospace
† AIAA Sr. Member, also Sr. Manager, The Boeing Company
‡ AIAA Associate Fellow, also Associate Technical Fellow, The Boeing Company
§ AIAA Fellow, T.V. Jones Professor of Engineering

Aerodynamics Team

Eric Ahlstrom, president of Star Aerospace LLC was responsible for the conceptual vehicle design and the preliminary aerodynamics. Based on the Mach limits, Reynolds numbers, and drag requirements of the concept a team of applied aerodynamicists with experience in state of the art transport aerodynamics was chosen for the detailed aerodynamic design and analysis. The aerodynamics team led by Robert Gregg and including John Vassberg, Dennis McDowell, and Mark DeHaan refined the design. CFD solvers and optimization methods as well as additional support were provided by Prof. Antony Jameson (References 1-7).

Design Objectives

The ideal Unlimited racing aircraft would extend the performance envelope to the limits of current propeller technology; Mach .80 and 35 HP/ft^2 of propeller disk area. Reliability should allow not only several races per year, but also several hours of practice time at each race without failure. In the coming years, the race schedule may be expanded to 6 to 10 events. To do this, the engine must be reliable, light, and powerful enough to last an entire season without failure.

The following is a list of requirements and limitations agreed upon by Renaissance Research and Star Aerospace LLC for the development of the G-Force Unlimited race aircraft.

1. Performance (all performance projected at 5,000' MSL, ISA +20°C)
   a. ≥600 mph TAS top speed in level flight.
   b. ≥550 mph lap speed on the 1999 Reno Unlimited air race course: 19% at 1 G, 60% at 4 to 6 G, and 21% in transition.
   c. 9 G maneuver load, 5 G gust load; total 14 G limit load factor with 1.5X safety factor to ultimate load failure.
   d. $V_{ne} \geq 550$ KEAS.
   e. $M_{mo} \geq 0.80$.
   f. Roll rate > 200°/sec at 350 KEAS.
   g. Stall speed < 90 KEAS.
   h. Landing distance < 1,500 ft., dead stick.
2. Schedule
   a. 1 prototype aircraft with spares sufficient for 10 race or air show events tested throughout the performance envelope and delivered race ready in 24 months from date of contract award.
   b. Production aircraft lead time of less than 12 months following completion of prototype testing, building to a rate of 2 aircraft per year.

It is interesting to note that the requirements for sustained turn rate and V_{ne} exceed those of some state of the art jet fighters.

Design Requirements

The design limitations, requirements, and assumptions are;

1. Piston powered and propeller driven (this is the only real rule in Unlimited Air Racing!)
2. Engine power/weight ratio: for reliability at continuous output, a limit of 2.5 HP/lb. was set for a modern turbocharged piston engine and gear reduction package with all accessories.
3. Stability and control
   a. Manual, unboosted control system.
   b. Positive static and dynamic stability greater than current Unlimited race aircraft.
   c. Minimal change in stability, power on vs. power off.
   d. Minimal change in CG and handling qualities, single vs. dual pilot.
4. Crew provisions
   a. Dual pilot, tandem seating, dual control for race training and PR flights.
   b. Low altitude ejection or pilot extraction systems for both pilots.
   c. 30° reclined angle for G tolerance.
   d. Provisions for mil spec oxygen and G-suit connections.

Course Analysis

An analysis of the Reno Unlimited race course yielded an optimum turn radius of about 1 mile for all three turns. These turns comprise over 70% of the race course. The differential between the pylon-to-pylon distance and the projected ground track will cause the aircraft to travel a minimum of 4% farther than the measured lap distance. Given the lap speed requirement of over 550 mph, the requirement for a sustained turn rate of 9.1°/second or 4 G was set at 550 mph. The increase in speed on the small straight areas of the course was calculated to approximately offset the 4% extra distance in the turns. Turbulence and other aircraft typically increase G loads to 2 or 3 times normal maneuver loads.

The 1999 and 2000 racecourses are illustrated below in Figure 1. The 1999 pylon to pylon lap distance was 8.3 miles. In 2000, the pylons before and after the finish line were moved to make the turns more uniform. The "deadline" at the south edge of the course was moved in to the north side of the runway. These changes were made to reduce the G required for a given lap speed and improve spectator safety. No changes were made to the program specifications.

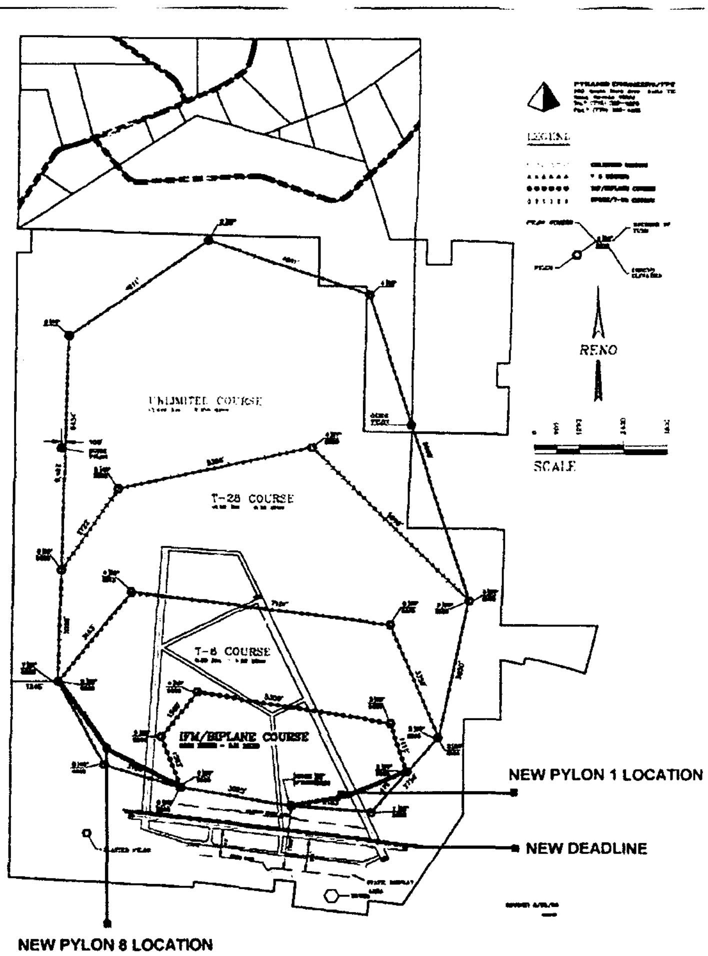

Figure 1 – 1999 & 2000 Reno Race Course

Conceptual Design

To satisfy these requirements, Sam Bousfield of Renaissance Research developed a preliminary configuration based on a mid fuselage or body propeller system.

The body propeller concept originated in the early era of aviation development to provide energized airflow over the tail surfaces and places the heavy engine, gear reduction, and propeller weights closer to the aircraft center of gravity. Its use was abandoned due to mechanical complexity in 1924. Inventor Sam Bousfield has developed several innovative methods to reduce the mechanical complexity required and has sponsored research into the performance potential of a body propeller equipped aircraft for both racing and civil use. Patents on these applications are pending.

The body propeller configuration allowed a very low fuselage wetted area and provided the potential for significant laminar flow over the forward fuselage. Engine size was chosen to provide about double the thrust to weight and thrust to wetted area ratios of the current Unlimited record holders, Rare Bear, Tsunami, and Dago Red.

Fuselage Design

The fuselage was lofted as a minimum volume fairing around the required propulsion system. Due to the 80" length and 40 to 50" width of the engine package, a wide forward cockpit was guaranteed and the addition of a second cockpit posed virtually no aerodynamic or structural penalties. The fuselage was lofted with a fineness ratio of 5.7, which later proved to be too aggressive. The pressure recovery in the region of the body propeller was tailored to provide an area of decelerated flow to the propeller and improve propulsion efficiency at transonic speeds.

Good structural layout was provided by locating the engine in the upper half of the mid fuselage, the wing below, and the cooling systems faired into the lower fuselage. The fuselage has been designed to be all composite forward of the firewall; composite shell with a structural sub frame in the engine area for maintenance access; and all composite aft of the body propeller. Primary bending loads will be carried through twin keel beams under the wing. All tail loads will be carried through the body propeller gearbox.

The propulsion system mass fraction of 42% centered in the fuselage provided for minimal CG change with different pilot weights and fuel loadings. Both crew positions were provided with sufficient room for SKS-94 type pilot extraction systems reclined 30° for G tolerance.

Conceptual Wing Design

Reference wing area was set at 75 ft^2 to provide a wing loading range of 40 to 46 lb./ft^2. Despite the high dynamic pressure of the racing environment and the opportunity for very high wing loading, the lower wing loading was necessary to provide a slow stall speed for safe dead stick landings. Based on cost and schedule constraints, a simple high lift system of single fowler flaps without a leading edge device was chosen. This allowed the potential for significant laminar flow, although the design for M_{dd} and structural thickness would have priority. Unit Reynolds numbers encountered during racing would range from 3 to 4.5M per ft. This gave wing Reynolds numbers of up to 20M at the wing root and 9M at the tip, comparable to a larger aircraft at higher altitude.

The maneuver loads, sustained turn rate, and the gust load required no buffet at a C_L of 0.64 at M 0.72; an M_{dd} of 0.75 at a C_L of 0.3; and an M_{dd} of 0.80 at a C_L of -0.05 to 0.1.

A trade study of wing thickness, sweep and taper ratio was made using NASA SC(2) airfoils as a baseline. From this, a section thickness minimum of 13.5% at the wing root and 12% at the tip was chosen combined with a quarter chord sweep of 28° for the M_{dd} specification of M 0.80. An aspect ratio of 8.3 and a taper ratio of .45 were chosen to allow a wing extension if race testing determined a need for it. Conversely, a production break was included in the wing at ~87% span to allow a reduction in the wing area by 4 ft^2, yielding an aspect ratio of 7.5. These adjustments will be used for different race courses where either more or less turning capability is required.

A planform Yehudi was incorporated into the wing trailing edge to provide space for the main landing gear. Because of the prop location and diameter, a fairly long gear length was required for propeller clearance. Later lengthening of the fuselage required the Yehudi to be blended with the outboard wing to provide more gear length. The Yehudi had the added benefit of reducing the wing downwash angle leading into the propeller.

The wing is a two-spar design with spars at 15 and 65% reference chord. A secondary spar behind the main gear-well parallels the Yehudi trailing edge and structurally supports the gear pivots. One-piece wing box construction will be used to reduce weight and complexity.

Conceptual Tail Design

To provide prop strike protection, the vertical stabilizer was located below the tail cone. With high-dihedral horizontal stabilizers in the normal position, this provided a Y-tail configuration. Additional benefits are that the vertical stabilizer becomes more effective at higher angles of attack and is not blanked by the fuselage or horizontal stabilizer in a stall or spin.

Tail sizing was set to provide approximately double the power on stability of a P-51. This was considered necessary due to the turbulent conditions of the race course and feedback from experienced pilots.

Configuration Concepts

A comparison study was made of the body prop design vs. the more conventional tractor and pusher configurations for the mission of Unlimited air racing. For the same wing loading and engine requirements, the study showed the body propeller configuration allowed the lowest wetted area, lowest drag, and highest propulsion efficiency for the required single engine, single propeller configuration.

Body Prop Design -

Figure 2 shows an inboard side view of all of the primary systems of the body prop equipped Unlimited racing aircraft illustrated for volume and balance. It is clear from this view that the body prop allows a compact and aerodynamic arrangement of engine, propulsion, structure and cockpit. The location of the wing spars, engine, and cockpit in close proximity allows the shortest load paths and the lightest structure. The fuselage illustrates a 24" stretch in the aft engine area over the original conceptual design to increase the wings critical Mach number (See discussion in Wing Design Section). This leaves a great deal of unused space between the engine and body prop. The exhaust and turbocharger installation may be moved into this area to improve engine accessibility. The engine block would be moved forward 6" to compensate for the CG change. Even so, this would provide 4 to 6" more room in the aft cockpit to carry instrumentation or recline the aft pilot for higher G tolerance. The proposed new turbocharger and engine arrangement is illustrated in the pusher version below.

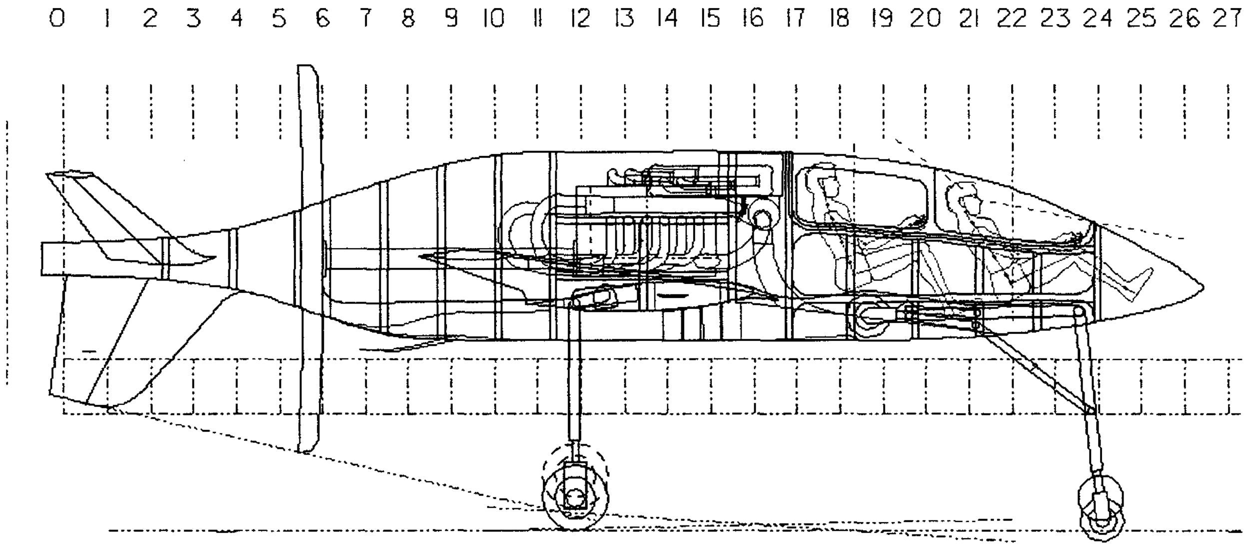

Figure 2 – Body Prop Aircraft Profile

The body propeller provides a very low drag design by allowing a laminar flow fuselage and wing. On takeoff, the prop accelerates the airflow over the tails providing positive control earlier than is possible in a pusher. The location of the prop near the CG provides a very small change in stability and handling qualities power-on vs. power-off. Finally, by profiling the fuselage at the body prop interface for a high degree of pressure recovery, the body prop can be made to fly in slightly decelerated air. This allows a higher advance ratio before the prop exceeds Mach limits and can be a large performance advantage at transonic speeds.

Mid-engine Pusher Design -

The mid engine pusher configuration is shown in Figure 3 and was derived from the body prop design by freezing the design forward of the wing trailing edge and changing only the propulsion and tail. This enables the pusher to share many of the advantages of the body prop version and use much of the same tooling. The forward fuselage can achieve significant laminar flow; the mid mounted engine provides low pitch and yaw inertia; and the aft cockpit has excellent visibility. The aircraft is longer than the body prop version and has more wetted area in the fuselage due to the large aft prop spinner. The tail has been moved forward and enlarged to maintain the same power off stability as the body prop version. The pusher prop is located further aft of the CG than the body prop, so the power on vs. power off stability change is greater. The CG impact of the aft propeller can be compensated for with either a more forward engine mounting or ballast.

The mid-engine pusher thrust line was set to keep the aft lower fuselage pressure recovery within airflow separation limits. The landing gear length is restricted by the wing design, so a full size-racing propeller would require a tailskid and/or main gear skid to prevent tail strike on landing. Alternately, a higher propeller disc loading could be used and diameter reduced.

The larger tail and increased fuselage wetted area account for half of the performance difference between the pusher and body prop versions. The other half of the performance difference is due to the lower flow deceleration available to the pusher at the propeller.

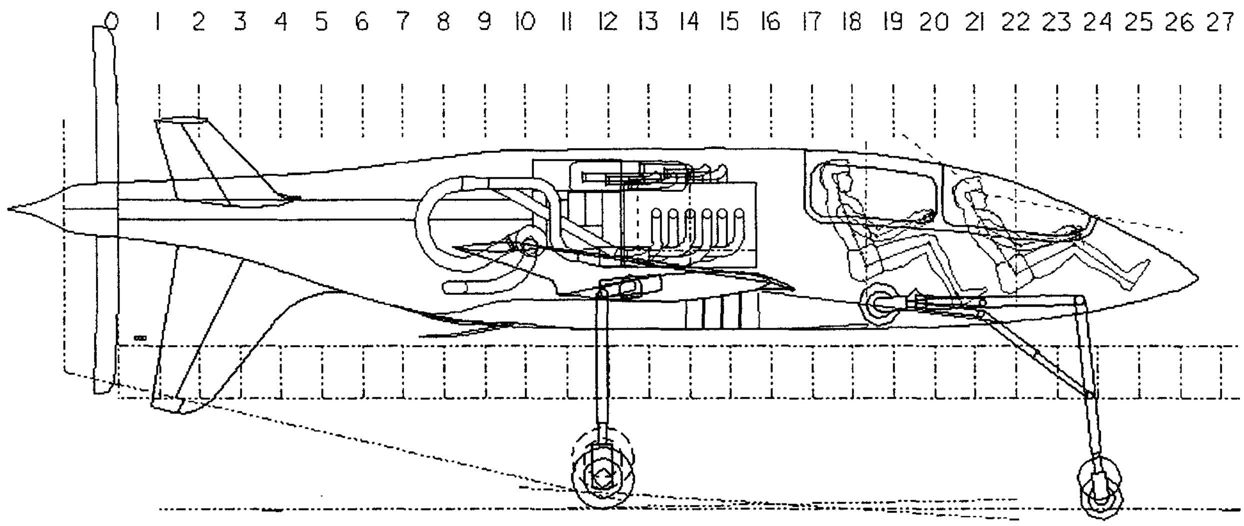

Figure 3 – Mid-engine Pusher Aircraft Profile

Tractor Design -

The tractor layout shown in Figure 4 is the most traditional aircraft configuration and is the most mechanically convenient. Placement of the engine, gear reduction, and propeller at the front of the aircraft allows the simplest mechanical design and best engine

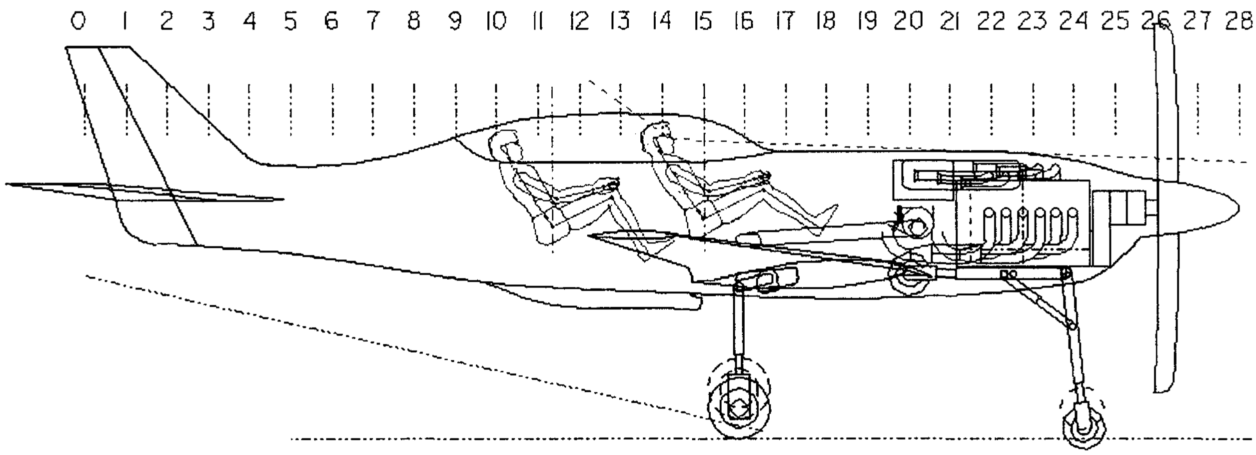

Figure 4 – Tractor Aircraft Profile

accessibility. The tractor prop placement allows the shortest landing gear length and reduction of the internal volume required for the retracted gear. A belly scoop cooling system was incorporated and did not account for a significant drag difference from the internal cooling systems of the body prop or pusher.

The tractor is the longest of the three configurations due to the high polar moment of inertia caused by the forward engine placement and the negative stability impact of the forward propeller. To keep the tail area within drag limits required a longer fuselage, which reduced the size of the tail surfaces and the total wetted area. A reduction in fuselage width aft of the engine combined with the canopy extension for the aft cockpit served an area ruling function. These factors improved wing root critical Mach number over the mid engine designs. However, the accelerated flow from the propeller increased the local Mach number at the wing root by the same amount so there was no net improvement. The entire fuselage is in turbulent flow and cannot be made laminar.

The tractor requires the largest tail volume of all three configurations and has a large stability change power-on vs. power-off. It should be noted that all of the current tractor Unlimited racers are experiencing some amount of yaw instability at race speed due to the stability derivative of the forward propeller. 28% of the performance shortfall of the tractor configuration vs. the body prop is due to the increased wetted area and the other 72% is due to the decrease in propulsion efficiency and the increase in fuselage drag due to the turbulent, accelerated flow and fuselage pressure drag from the tractor propeller.

Propeller Considerations

The body propeller looks radical, yet the concept of a prop on a body of revolution operating at transonic conditions has been well proven. The integration of a transonic propeller in the aft third of the fuselage proved to be very similar to the MD-80 and Boeing 7J7 UnDucted Fan (UDF) engine nacelles of the late 1980's. The MD-80 UDF demonstrated excellent efficiency and performance up to Mach 0.8. The UDF concept was eventually dropped as a result of fuel prices not increasing as projected in the early 80's. This concept would have likely been introduced into a production aircraft design had fuel prices remained high.

Even at speeds of Mach 0.75 to 0.8, a body propeller driven by a turbocharged piston engine exceeds the efficiency of the best fan jets. This makes the body propeller design the best choice for the next generation of Unlimited racing aircraft.

Prop diameter is a primary driver of both propulsion efficiency and aircraft stability. A tractor aircraft requires the shortest landing gear for a given propeller diameter, but suffers the greatest stability loss. The pusher gets the greatest stability enhancement from the propeller in the power-on condition, but loses this benefit power-off. A large propeller on a pusher aircraft can make the landing gear so large as to be impractical. With its location near the CG, only the body prop aircraft combines minimal stability change with acceptable gear length.

Both the body prop and pusher designs are mid-engine, and allow radical changes in engine weight and volume without significant changes to the airframe. This makes either design a viable choice for new engine development. The tractor design would require new aero structure and ballasting to allow any significant change in engine weight or volume.

The performance comparison, shown in Table 1, shows that the body prop could be capable of breaking the existing prop driven speed records on a power rating of 1500 HP, while the pusher would need 1800 HP; the tractor design would barely scratch the current records at 2200 HP.

Comparing lap speeds, we note that the pusher requires *22% more power for the same average lap speed.* The tractor needs *47% more power to go 5 mph slower* than the body prop.

Dimensions	**Mid-engine Body Prop**	**Mid-engine Pusher**	**Front-engine Tractor**
Empty weight	2,754 lb.	2,956 lb.	2,794 lb.
Fuel capacity	83 gal.	83 gal.	83 gal.
Race takeoff weight	3,454 lb.	3,656 lb.	3,494 lb.
Length	27 ft.	28.5 ft.	29.5 ft.
Wing span	25 ft.	25 ft.	25 ft.
Wing area	86.9 ft^2	86.9 ft^2	86.9 ft^2
Wetted area	437 ft^2	473 ft^2	460 ft^2
Aspect ratio	7.2	7.2	7.2
Wetted aspect ratio	1.42	1.31	1.42
Aft cabin width	52"	52"	< 35"
Performance at Reno, NV; ISA +20C	**Mid-engine Body Prop**	**Mid-engine Pusher**	**Front-engine Tractor**
Piston-prop level speed record			*541 mph*
Level speed, 1500 HP	529 mph	508 mph	482 mph
Level speed, 1800 HP	564 mph	538 mph	511 mph
Level speed, 2200 HP	606 mph	578 mph	547 mph
Piston-prop lap record			*492 mph*
Lap speed, 1500 HP	503 mph	483 mph	458 mph
Lap speed, 1800 HP	525 mph	500 mph	475 mph
Lap speed, 2200 HP	551 mph	526 mph	498 mph
Max L/D (glide ratio without propeller)	17.9	17.2	13.4

Table 1 – Performance Comparison of Configuration Concepts

Configuration Refinement

This section covers the refinement of the various components of the aircraft. For the purposes of the paper, discussions regarding each component are split into different sections.

Wing Design –

Any successful system design effort must accommodate a changing set of requirements as the designers of the various subsystems learn more about how their individual efforts impact and are affected by the actions of the other designers. This was certainly the case with this wing design as we integrated it with the fuselage, propulsion system, stability & control, manufacturing and overall packaging. Most of the assembled team has worked closely together for more than a decade. Our style has been to allow the individuals of the team to gravitate towards the work items that they feel most comfortable with, however, each member will loosely participate in all concurrent activities in progress. This participation is usually in the form of daily discussions regarding the overall design of the aircraft. By disseminating everybody's findings on a very frequent basis, the group as a whole begins to understand how best to maximize the system's performance, even if it means taking additional compromises at the subsystem levels. These informal design reviews also serve the purpose for sanity checks to occur frequently enough such that a poor design direction is not ventured too far.

Another characteristic of this group is that we have been programmed to work on tight schedules and under small budgets. As a result, you will notice that the group utilizes the most cost-effective tools at every stage of the design effort. Initially, when the design is not very well understood, design charts and rules-of-thumb dominate the effort. As the design begins to evolve, and these methods no longer add value to the direction of the group, linear methods are drawn into the tool set. Then, as the ROI of linear methods begins to reduce, they are replaced by non-linear tools - starting with the simple and finishing with the most sophisticated. Using the right tool at the right time helps us manage costs and schedule, and allows our final designs to be competitive at the highest level.

The design of the wing geometry occurred in several phases, with the basic requirements defined by Ahlstrom in phase I. These requirements included the general layout (planform, thickness distribution) of the wing, the design cruise condition (M=0.77, C_{Ltot}=0.32, Ren=14.5M), off-design capabilities ($C_{Lbuffet}$=0.64 at M.72, M_{dd}=0.80 at C_L=0.1, C_{LmaxCW}=1.6, etc.), and a pad on the divergence Mach number to allow room for growth in out years. McDowell verified that the original planform sweep and thickness combination was appropriate for the desired Mach number capabilities of the race course mission; this was done with design charts.

The baseline wing of phase II was defined by Gregg, McDowell & Vassberg using airfoil sections derived from NACA 64 sections, scaled to conform to the original planform and thickness distribution established in phase I. Some cursory 2D optimizations were performed on these sections to better tailor their characteristics for the initial design conditions; the 2D conditions and geometry transformations used for this effort were based

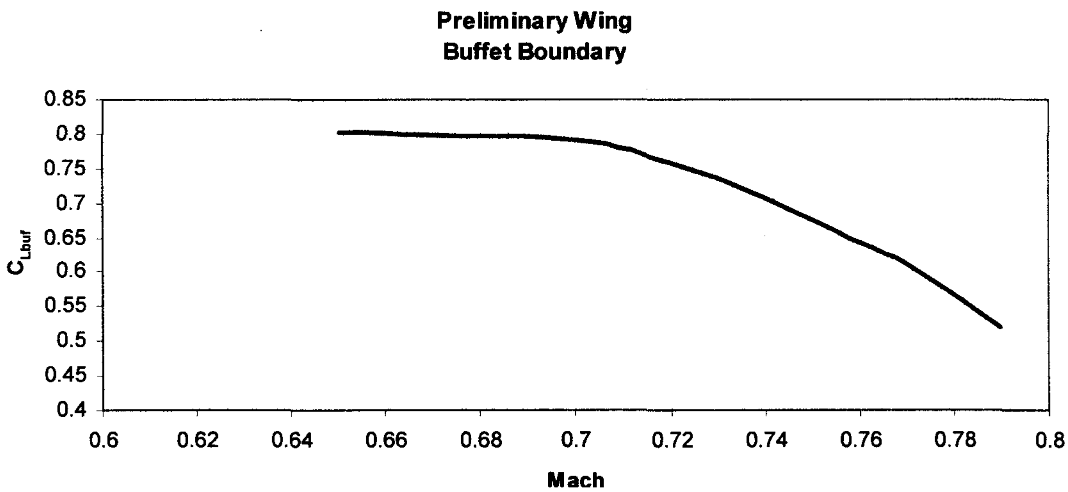

Figure 5 – Preliminary Wing Buffet Boundary

on simple-sweep theory. The method used for this 2D activity was Jameson's SYN103 code run in Euler, drag-minimization mode. At this point, the remaining unspecified geometric quantity was the twist distribution of the wing. To set this, we utilized Jameson's FLO22 wing-only code, but we included pseudo-fuselage effects. The first pseudo-body influence is its acceleration on the on-set Mach number at a critical station on the wing; typically this is around 50%-60% semi-span. Running the isolated fuselage geometry in a surface-panel method and interrogating the flowfield velocity at the critical wing station determine this acceleration. The second pseudo-body effect is how the presence of the fuselage at an angle of attack warps the on-set flowfield's local angle of attack as a function of span location. The third pseudo-body influence is related to the carry-over lift of the wing's circulation onto the fuselage. This ratio is defined as C_{Ltot}/C_{Lwing}, is 1.22 for the G-Force configuration and was determined by running a surface-panel method on the wing/body combination. These pseudo-body effects are included in FLO22's wing-only solution by running the exposed wing in the code at the wing's C_L, at a higher Mach number and re-referencing the results back to the original Mach, and adding a delta-twist distribution to the wing to simulate the flowfield warping. Using this procedure, we specified a twist distribution that yielded a near-elliptic span loading. This initial design was done very rapidly, covering only a two-day period of after-hours work. It provided us a point to start the 3D design effort. For reference, FLO22 runs in about 7 seconds on an AMD Athlon 800 MHz powered PC.

The initial analysis indicated that the design requirements could be satisfied with a thicker wing than the conceptual layout of Ahlstrom. Some additional margin in buffet boundary, cruise Mach number and M_{dd} was felt desirable to provide an additional margin for aileron effectiveness at these speeds. Figure 5 presents the initial buffet analysis of the wing configuration as estimated by FLO22 at this stage of the design. Table 2 shows the

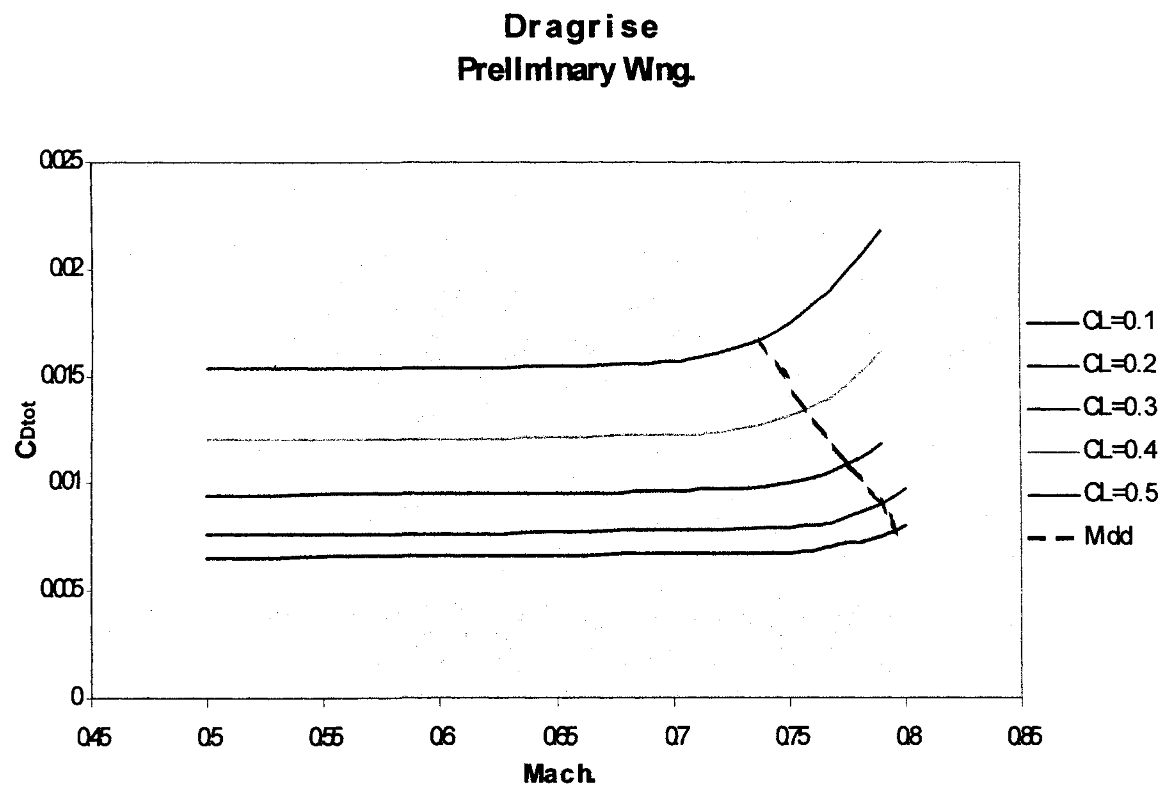

Figure 6 – Preliminary Wing Dragrise

C_L	M_{dd}
0.1	0.796
0.2	0.790
0.3	0.775
0.4	0.757
0.5	0.738

Table 2 – Preliminary Wing Mach Capability

estimated Mach capability at different C_L's, while Figure 6 shows the drag rise characteristics. All of this analysis indicated that requirements were being met, however there was a serious concern with the body effects on this low fuselage fineness ratio configuration. The dragrise characteristics indicate that this initial wing had a Mach capability at $0.3C_L$ of about 0.775; however, this estimate was shown to be optimistic due to the pseudo fuselage correction used in this analysis.

Without worrying too much about it, the team was relatively sure that our baseline wing was going to have problems near the root region because of the atypical contouring of the fuselage geometry, thus began phase III that was conducted by Vassberg & Jameson. The first thing to do was to assess what issues might exist with the baseline wing geometry (designated shark1), as it integrates with the fuselage. This analysis was performed on 9 NOV, 1999 using Jameson's SYN88 Euler method and is illustrated in Figure 7. The quantities in the legend of this figure correspond to the wing forces. Furthermore, the drag listed is only the inviscid drag, which includes the induced and shock components. If you will recall, the design lift was C_{Ltot}=0.32 and that the carry-over lift ratio was 1.22 for this configuration. Hence, the wing lift is C_{Lwing}=C_{Ltot}/1.22=0.27. The other item to note is that this analysis was performed at a Mach number of M=0.78 rather than M=0.77. The reason for this bump in freestream Mach number was due to the on-set acceleration of the flowfield near the wing root from the

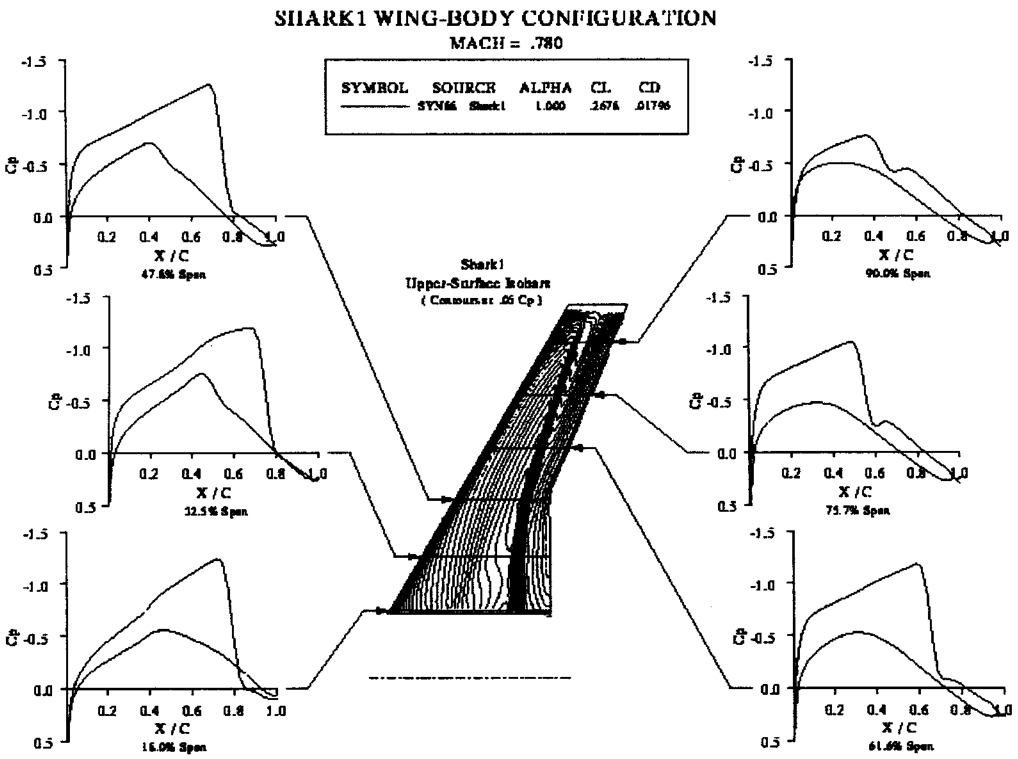

Figure 7 – Shark1 Wing/Body Pressure Distributions

propulsion system. McDowell & DeHaan using methods based on actuator-disc and blade-element theories determined this acceleration. Since we were concerned most about the wing-root region at this stage in the design, we used the full level of propeller effects on the on-set Mach number. Referring to Figure 7 again, notice the strong shock that unsweeps as it nears the side-of-body. As we had suspected, the contouring of the fuselage cross-sections had an adverse effect on the wing aerodynamics, unfortunately it was worse than we had feared. The inviscid drag (induced + shock) of the wing was $C_{DwingINV}$=180 counts for the baseline configuration. For reference, SYN88 and a drag-minimization run with thousands of design variables uses about 10X the CPU time of an analysis calculation.

Phase III continued by running SYN88 in drag-minimization mode, constraining the wing modifications to be thicker everywhere than the baseline geometry. Initially, we were running these optimizations at a single point (cruise design), just to see what the potential benefit might be. Within 30 design cycles, SYN88 dropped the wing's inviscid drag from 180 counts to 104 counts. This optimization was launched on the evening of 9 NOV, 1999 and completed early 10 NOV, 1999… an over-night turn-around. Although fairly large improvements were realized, we felt we could do better if we were allowed to modify the fuselage contour near the wing trailing edge. In discussions between Gregg, Ahlstrom, McDowell, Vassberg & Jameson, several concurrent changes to the aircraft's general layout were being considered. The team was forming these ideas as we were beginning to learn more about the complete system. The changes that were directly related to the wing design were the fuselage reshaping and a trailing-edge planform blending that would allow more room for stowing the landing-gear structure. Gregg & Vassberg made the planform modifications to the current wing and

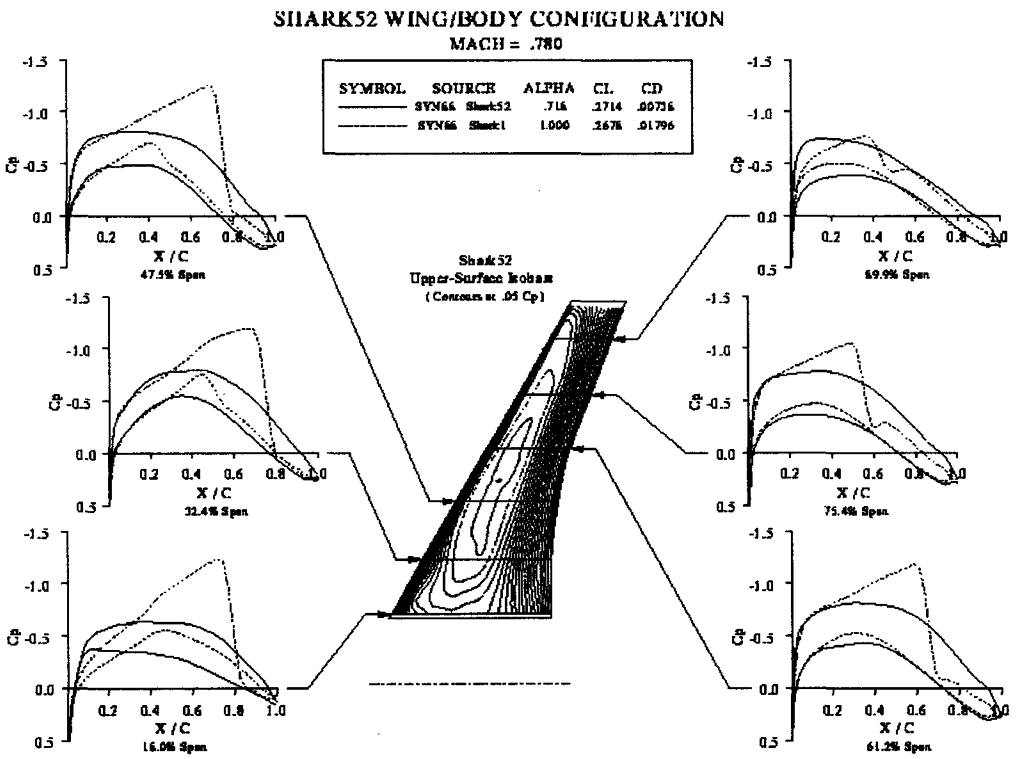

Figure 8 – Shark52 Wing/Body Pressure Distribution

Vassberg simultaneously generated an additional three fuselage definitions that parametrically stretched it by 1, 2 and 4 feet aft of the wing-root mid-chord and consistent with the engine packaging requirements. Other fuselage geometries were created, however they were not pursued because the fuselage stretching exercise achieved our goal to essentially eliminate the unsweeping of the shock system at the wing root. In fact, the trailing-edge modification was also done in a manner to help alleviate the shock-unsweep problem; as well as accommodate the landing gear. This planform change proved to be beneficial as another triple-point drag minimization was performed on 13-14 NOV, 1999, which dropped the wing's inviscid drag from 148 counts to 98 counts at the design point. For clarification, this wing redesign was done with the original fuselage to establish a new base for the parametric study, which stretched the fuselage. Repeating similar triple-point optimizations on the 1-, 2- and 4-foot fuselage extensions provided sufficient data to show that we could completely eliminate the shock unsweep with the 2-foot stretch. This optimization reduced the wing's inviscid drag from 92 counts to 72 counts within 30 design cycles; the resulting wing geometry was designated shark52. The pressure distribution for shark52 at M=0.78 and $C_{L_{Wing}}$=0.27 is shown in Figure 8. It should be emphasized that within the course of one week, the wing geometry had evolved from one that produced 180 counts of inviscid drag to shark52, which only has 72 counts at the design point. This is an extremely large improvement accomplished in a very compressed time! Furthermore, the database of CFD solutions (~100) had grown large enough that very informed modifications to the configuration could be made. This included the wing-planform change to better stow the landing gear, as well as the fuselage reshaping to eliminate the shock unsweep issue. Figure 9 shows a side-by-side comparison of the pressure isobars of the initial wing and the shark52 wing that clearly shows the reduction

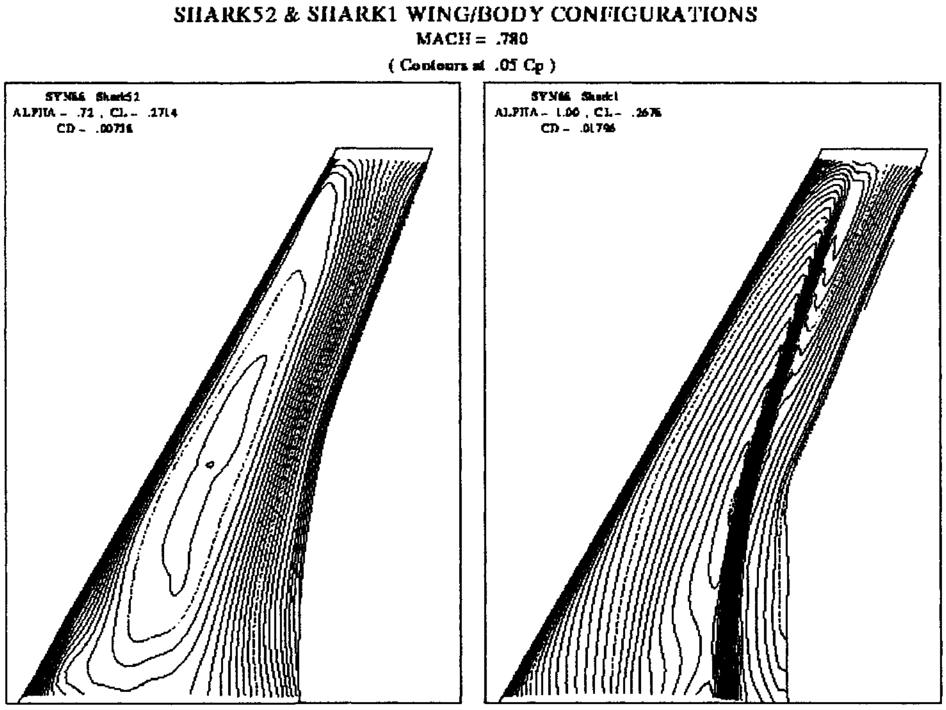

Figure 9 – Comparisons of Initial and Final Wing Pressure Isobars

in the shock strength across the entire wing, as a result of all of these important changes to the configuration. The final aspect of phase III was that we needed to rebalance the aircraft. This required a 6-inch stretch forward of the wing to compensate for the 2-foot stretch of the after-body. Once the fuselage geometry was frozen, we polished the pressure distributions some more by running SYN88 in inverse-design mode.

Not much else was done on wing design for the remainder of 1999 because of Thanksgiving and Christmas holidays and other end-of-year commitments. However, the team began to kick around the idea of a laminar-flow design. We did some quick calculations on the attachment line Reynolds number, Re_θ, of the current wing and discovered that we were within the range where Tolmin-Schlichting waves along the attachment line would decay rather than amplify. So we felt that the possibility of laminar runs was achievable. The dilemma, however, was could we count on getting laminar flow in the field. After all, this is a race plane whose mission is at very low altitude above ground level where bug strikes are sure to occur. What we decided to do was to investigate whether or not we could tailor the wing's pressure distributions to have favorable gradients for up to 40% chord without adversely affecting the aerodynamic performance of the fully-turbulent wing design. If we could, then we would change the design, yet not take credit for any laminar-flow-related drag reductions.

Phase IV began in mid-January, 2000. This development was concentrated on promoting laminar flow on the wing without degrading the performance of the wing if it was fully turbulent as compared with the fully-turbulent design of shark52. This objective was not limited to the design point, but rather was expanded to include the Mach number range of M>0.74 and a lift range of $C_{L_{wing}}<0.27$. The first task was to compute the viscous flow about the shark52 configuration at various flow conditions. This was accomplished using

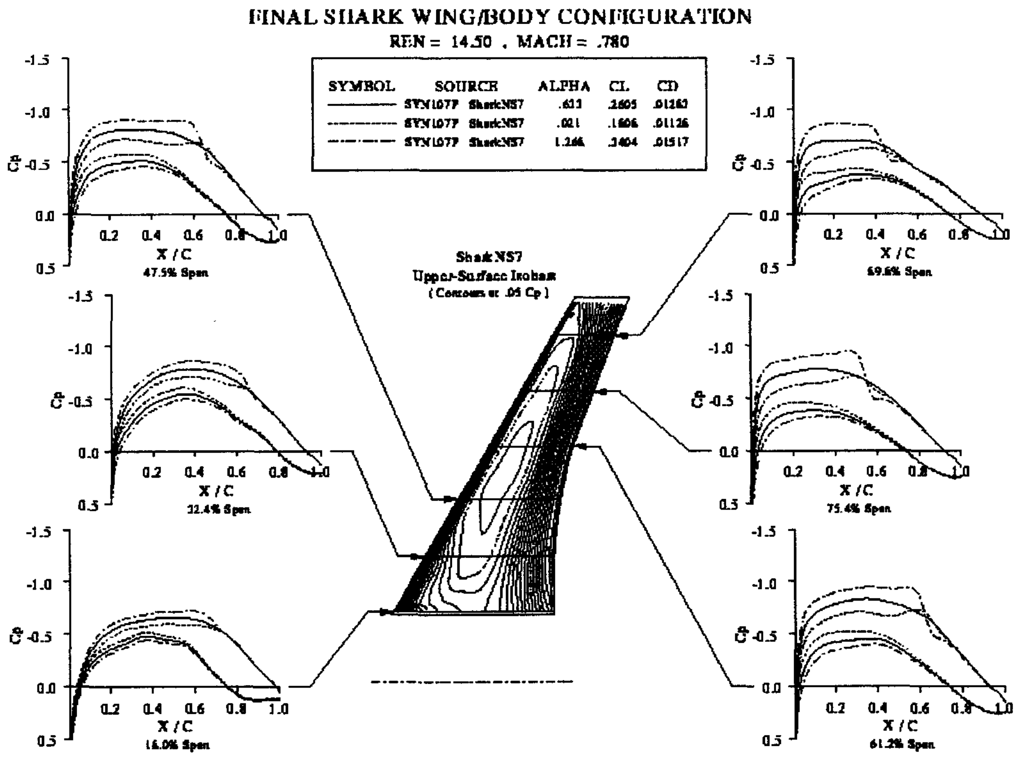

Figure 10 – Final Wing/Body Pressure Distributions

Jameson's SYN107P Wing/Body Navier-Stokes method. Starting with the computed pressure distributions of shark52, a series of inverse designs were performed, also with SYN107P. Vassberg & McDowell would modify the pressure distributions and Jameson & Vassberg would run SYN107P in inverse-design mode. The design Reynolds number was Re=14.5M, based on the reference chord. What we found was that it was easier to redesign the wing at the higher Mach number and accommodate the requirements at M=0.74, rather than the other way around. This study was completed on 8 FEB, 2000 with the wing geometry designated sharkns7. Figure 10 illustrates the pressure distributions for sharkns7 at M=0.78 and a lift range of C_{Lwing}=0.18-0.34. At the design point C_{Dwing} is 128 counts which is composed of $C_{Dwing\text{-}Form}$ =77 counts and $C_{Dwing\text{-}sf}$ = 51 counts. Note that favorable gradients exist on both upper and lower surfaces for about the first 30%-40% chord, depending on span location and lifting condition. For reference, SYN107P runs in parallel under MPI, and optimization runs cost about 10X-20X the cost of an analysis. Recent SYN107P benchmarks on a 16 processor Athlon 650 cluster shows the analysis running in 30 minutes.

For those unfamiliar with inverse design, we should point out that a pressure modification very near the leading-edge "stagnation" point could dramatically alter the leading-edge geometry. This occurred in the above exercise, which yielded a leading-edge radius distribution that was not smoothly varying out the span, yet this was expected. Hence, our final task of phase IV was to re-establish an appropriate leading-edge radius distribution without really changing the wing pressure distributions at the cruise design conditions. We tailored the wing's leading-edge geometry for low-speed characteristics as well as with consideration to the requirements needed for promoting laminar flow. These modifications were accomplished with local explicit geometry perturbations. During this leading-edge modification step, Ahlstrom and McDowell also slightly reduced the required wing thickness distribution. After both of these changes were incorporated into sharkns7,

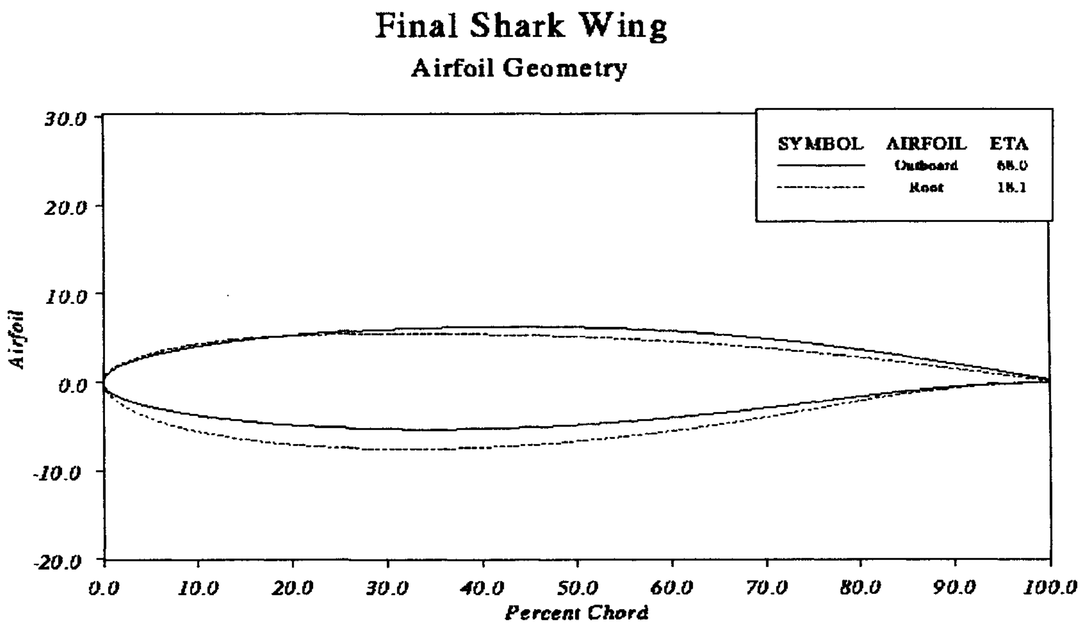

Figure 11 – Final Wing Root and Tip Airfoils

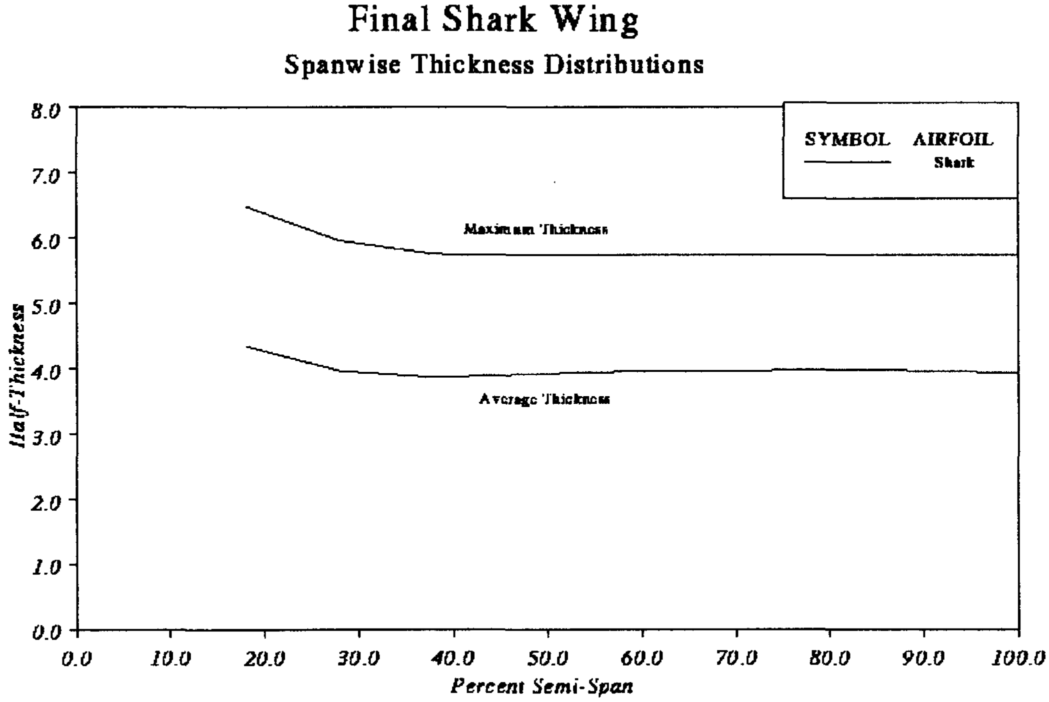

Figure 12 – Final Wing Half-Thickness Distribution

the final wing was analyzed to verify that these geometry changes did not adversely effect the pressure distributions. When overlaid on the same plot, the curves nearly appeared as one.

The final wing geometric characteristics resulting from the process described above are shown in Figures 11 and 12. Shown are the root and an outboard airfoil along with the half-airfoil thickness distribution across the span. As indicated in Figure 12, the maximum thickness averages around 12%. Overall, these numbers are not significantly different from what Ahlstrom had originally assumed in his conceptual layout of the G-Force configuration.

The estimated benefit of laminar run is between 10 and 20 counts of drag depending on the Mach number. On the lower surface, the positive gradient allows a laminar run to approximately 30 to 40% chord before the adverse gradient will cause transition. On the upper surface the shock will trigger transition provided any attachment line contamination from the fuselage boundary layer is removed by a notch-bump, and that the Re_θ does not exceed about 200. The leading edge Re_θ varies from approximately 125 just outboard of the fuselage to around 80 at the tip. The amount of laminar run on the upper surface will increase as Mach increases due to the shock moving aft on the airfoil as well as the pressure gradients becoming more favorable. As a result, it is expected that at race conditions the wing will have an appreciable extent of laminar flow provided that the surface of the wing is smooth and free of particulate contamination.

Clean wing C_{Lmax}, C_{LmaxCW}, was also monitored during the design process to ensure the wing satisfied the clean wing stall speeds required by Star Aerospace. The design requirements was to provide a C_{LmaxCW} of at least 1.6 at a Mach=0.2. This was determined by solving the flow field about the wing with FLO22 at a number of angle of attacks (approximately 15 to 16 degrees in most cases) and interrogating the wing to find C_{pmin} at various spanwise stations. When a critical C_{pmin} value (for this Reynolds number, C_{pmin} is approximately -15) is exceeded, C_{Lmax} is defined. The wing developed for the G-Force exceeds the C_{Lmax} requirement slightly, having an estimated C_{LmaxCW} of 1.64.

Tail Design –

An initial look at the horizontal tail sizing as determined by Ahlstrom indicated a larger horizontal tail was required, but after estimating the fuselage contribution to stability using CFD analysis instead of "cookbook" equations, McDowell & DeHaan determined that the tail was sized appropriately for this type of aircraft. From an aft C.G. of 30%, the aircraft is estimated to be 25.2% stable power-off and 33.2% stable at 550 mph and full power. The Neutral Point is estimated to be at 54.5% c_{mac}. Directional stability indicates that the G-Force configuration has over twice the direction stability of stock WWII fighters in use at Reno. The estimated $C_{n\beta}$ for this configuration is conservatively -0.002 power off and -0.00255 at full power. Typical WWII aircraft have a $C_{n\beta}$ of approximately -0.001 at normal operating power. This should provide an advantage for the G-Force aircraft as typical warbirds exhibit low directional stability at high speed racing conditions.

The final horizontal and vertical tails utilize modified NACA 4, 63 & 64 series symmetrical airfoils with a thickness of just less than 15% for the horizontal tail and 13% for the vertical tail. The tail Mach capability with these airfoils and with tail sweeps of 35 and 36 degrees (horizontal and vertical tails respectively) is estimated to be M=0.84. Two concepts to compensate for prop swirl are still being considered. One approach is to twist the tail for the estimated swirl distribution as determined by blade element theory. Defining a twist distribution on a symmetric airfoil tail still allows for a non-handed part by flipping the tail left to right. A second approach is simple to rig a slab tail asymmetrically to compensate for the swirl. Multiple tails are being considered for flight testing to determine the optimal configuration.

Fuselage and Prop Face Mach -

The local Mach number was evaluated at the prop disc plane (without the effect of the prop itself) by DeHaan using a surface-panel method (References 8-9). The analysis indicated that the propeller disc will see a Mach number that is 4% less than the freestream Mach number. For comparison, a prop at the front of the aircraft would see approximately the same freestream Mach number. Work was performed to try to further reduce the onset Mach number seen at the prop; some reductions were possible but at a trade of causing flow separation along the body near the prop. The concept of reducing Mach number at the prop disc by further fuselage shaping was dropped.

Drag Build-up -

A drag build-up for this aircraft was completed and indicates that the profile drag estimate for the G-Force during the conceptual phase is reasonable. Table 3 summarizes the estimated drag of the aircraft at race conditions of 550mph. Not included in this estimate is any laminar run on the body or wing. Therefore, approximately 5% better performance than these estimates is likely. Note that at this speed, max L/D occurs at 0.49 C_L (approximately a 7g case) and is estimated to be 14.78.

Table 3 – Estimated Drag Build-up

Condition	6000', 550 mph	6000', 550 mph
C_L	0.07	0.30
g's	1	4
C_{Do}	0.01928	0.01928
C_{Di}	0.00025	0.00462
C_{Dc}	0.00023	0.00054
C_{Dtrim}	0.00010	0.00012
C_{Dtot}	0.01986	0.02455
L/D	3.52	12.22

Conclusions

If Unlimited racing is to continue in the future as a viable and exciting sport, newly designed race planes are required to replace the aging, but beautiful, piston powered fighter aircraft of the 1940's. This paper describes the development of a new Unlimited Race plane, G-Force, designed to fly 550 mph laps at Reno. The processes utilized to develop this aircraft range from very simple to N-S Optimization tools. The combination of these tools, used efficiently and where each tool can provide meaningful results, under the eye of experienced engineers, rapidly developed a configuration that satisfied a set of well defined goals. It is interesting to note how accurately conceptual methods can be at providing global layouts of such specialized aircraft as the G-Force. However, without the use of optimization tools, such as SYN107P this wing design would not have been rapidly developed nor would it likely have satisfied all these requirements as well as it does.

Acknowledgements

The wing design effort would not have been as successful as it was without the participation and contributions of Antony Jameson of Stanford University. Professor Jameson supplied consulting time, aerodynamic design and analysis software as well as computer resources through his firm, Intelligent Aerodynamics, Int'l. The authors would also like to acknowledge The Boeing Company for allowing the aerodynamics team to work on this project after hours.

References

[1] A. Jameson. Transonic Potential Flow Calculations Using Conservative Form. Proceedings of AIAA 2nd Computational Fluid Dynamics Conf., June 1975, pp. 148-161.

[2] P.A. Henne and R.M. Hicks. Wing Analysis Using a Transonic Potential Flow Computational Method. NASA TM-78464, July 1978.

[3] A. Jameson, W. Schmidt, and E. Turkel. Numerical solutions of the Euler equations by finite volume methods with Runge-Kutta time stepping schemes. *AIAA paper 81-1259*, AIAA 24th Aerospace Sciences Meeting, Reno, NV, January 1981.

[4] A. Jameson. Solution of the Euler equations for two dimensional transonic flow by a multigrid method. *Applied Mathematics and Computations*, 13:327-356, 1983

[5] A. Jameson. The present status, challenges, and future developments in Computational Fluid Dynamics. Technical report, 77th AGARD Fluid Dynamics Panel Symposium, Seville, October 1995.

[6] A. Jameson. Optimum aerodynamic design via boundary control. In *AGARD-VKI Lecture Series, Optimum Design Methods in Aerodynamics*. von Karman Institute for Fluid Dynamics, 1994.

[7] A. Jameson, L. Martinelli, and N. A. Pierce. Optimum aerodynamic design using the Navier-Stokes equations. *Theoretical and Computational Fluid Dynamics,* 10:213-237, 1998

[8] J.L. Hess and A.M.O. Smith. Calculation of potential flow about arbitrary bodies. *Progress in Aeronautical Sciences,* 8, 1966.

[9] J.C. Vassberg. A fast surface-panel method capable of solving million-element problems. *AIAA paper 97-0168,* 35th AIAA Aerospace Sciences Meeting, Reno, NV, January 1997.